

A novel Cd₄O₄ cubane cluster-based complex and its bifunctional catalytic activity aiming for artificial photosynthesis

M. Sooraj, B. Haritha, S.N. Remello, E. Manoj*

Department of Applied Chemistry, Cochin University of Science and Technology, Kochi, Kerala 682 022, India

* Corresponding author.

E-mail address: manoj@cusat.ac.in (E. Manoj).

Sl. No.	Contents	Page no.
1.	Fig.S1. The crystal packing of complex 1 observed along the c-axis.	S3
2.	Fig.S2. Relevant hydrogen bonding interactions of complex 1 , in the lattice observed along the b axis, indicated by dashed lines.	S3
3.	Fig. S3. Overlay of the experimental and simulated PXRD patterns of complex 1 .	S4
4.	Fig. S4. Solution phase UV-vis spectrum of complex 1 in 10 ⁻⁴ M methanol solution.	S4
5.	Fig. S5. Experimental (top) and theoretical (bottom) IR spectrum of complex 1 .	S5
6.	Fig. S6. Experimental (top) and theoretical (bottom) Far IR spectrum of complex 1 .	S5
7.	Fig. S7. ESI-MS spectrum of complex 1 in methanol, showing relevant peaks.	S6
8.	Fig. S8. 2D fingerprint plots of complex 1 .	S6
9.	Fig. S9. Void surfaces of complex 1 arising from different isovalues (0.002 au (a) and 0.0008 au (b)) for a unit cell.	S7
10.	Fig. S10. DFT optimized structure of complex 1 .	S7
11.	Fig. S11. Molecular electrostatic potential surface of complex 1 .	S7
12.	Fig. S12. LSV control experiment for (a) water oxidation and (b) CO ₂ reduction activity of complex 1 .	S8
13.	Table S1. Interaction parameters of complex 1 .	S8
14.	Table S2. Hirshfeld surface properties of cadmium cubane cluster.	S8

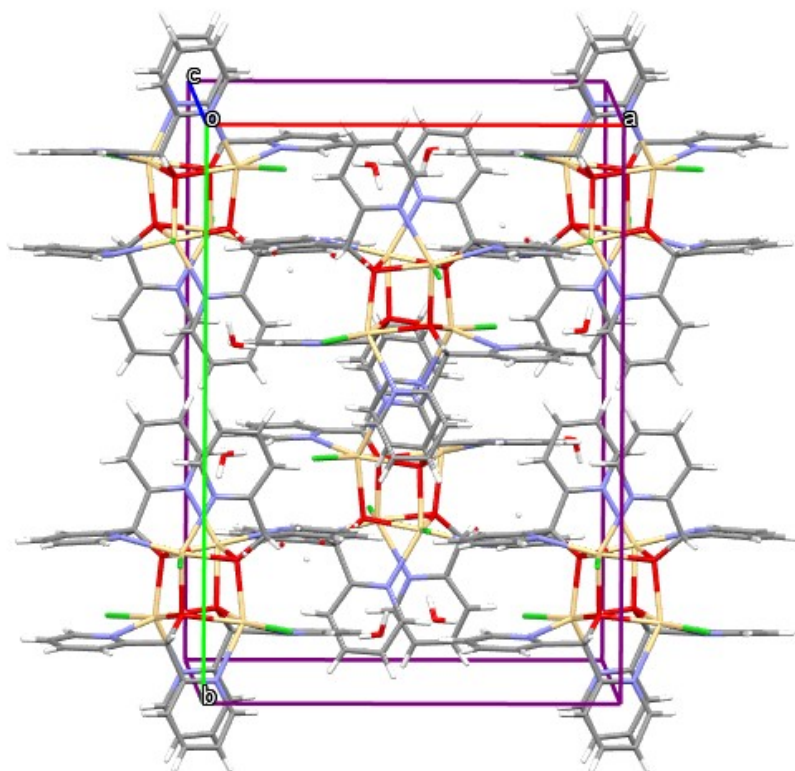


Fig. S1. The crystal packing of complex **1** observed along the c-axis.

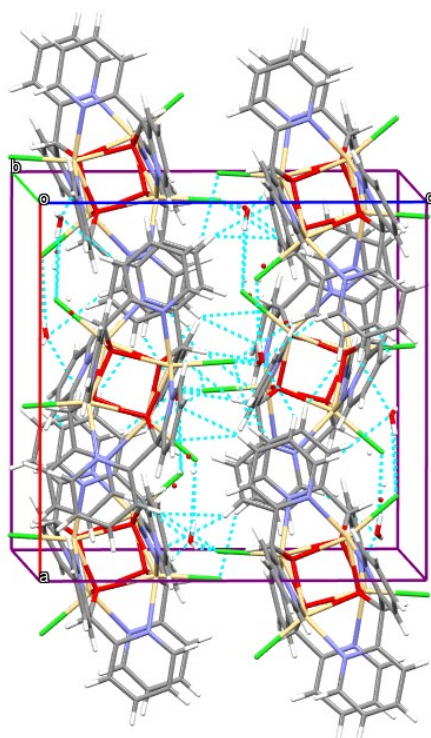


Fig. S2. Relevant hydrogen bonding interactions of complex **1**, in the lattice observed along the b axis, indicated by dashed lines.

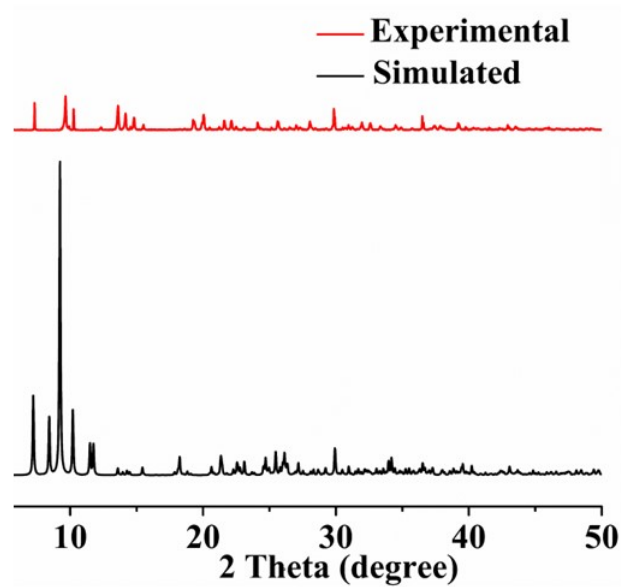


Fig. S3. Overlay of the experimental and simulated PXRD patterns of complex 1.

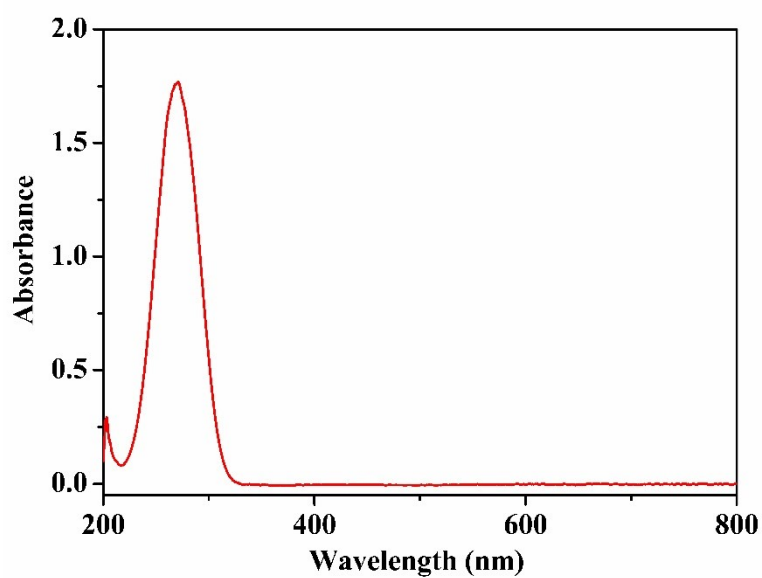


Fig. S4. Solution phase UV-vis spectrum of complex 1 in 10⁻⁴ M methanol solution.

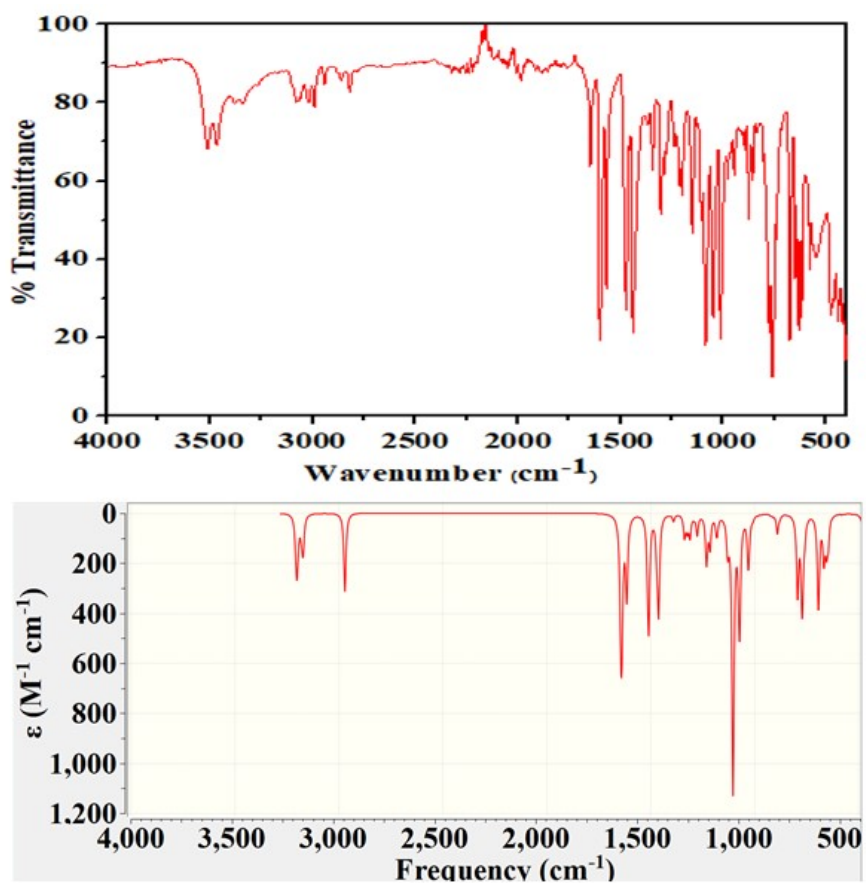


Fig. S5. Experimental (top) and theoretical (bottom) IR spectrum of complex 1.

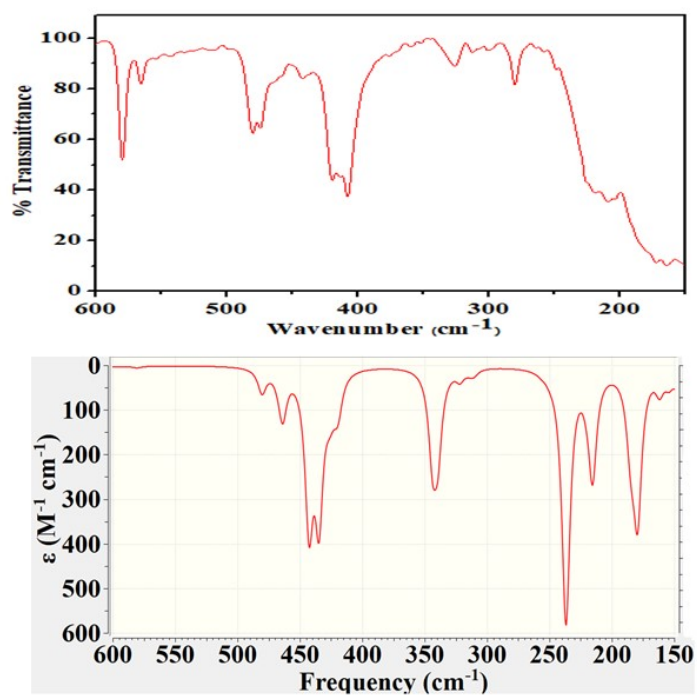
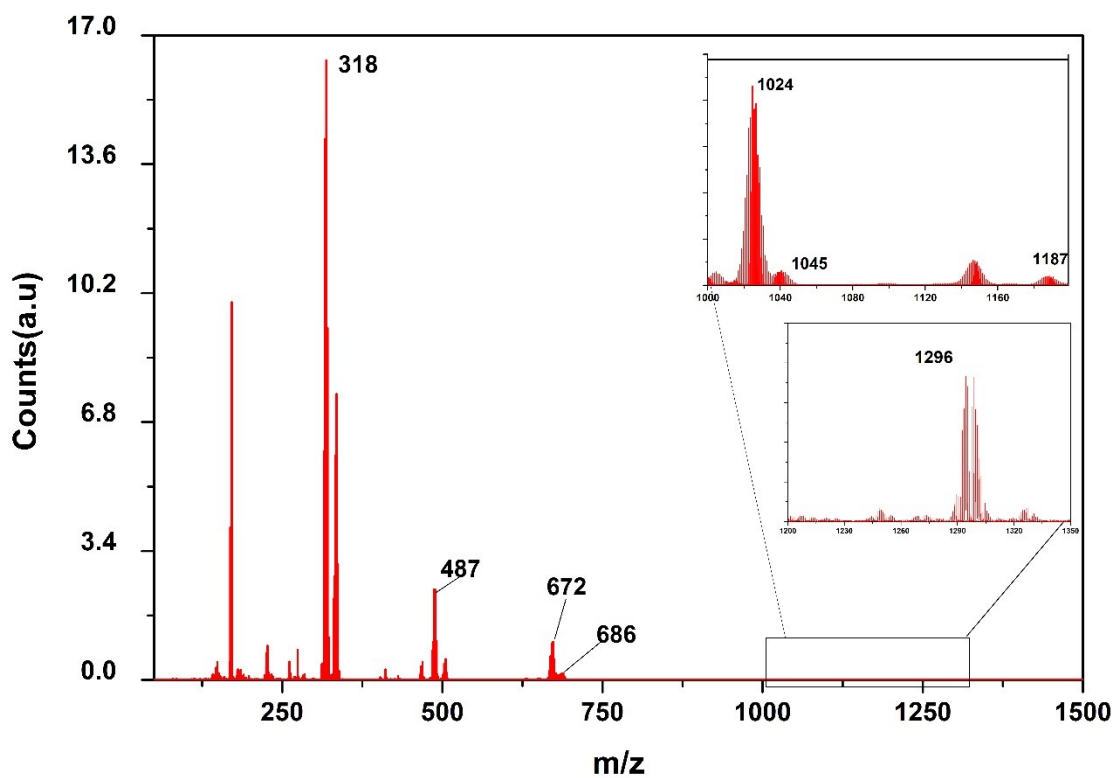


Fig. S6. Experimental (top) and theoretical (bottom) Far IR spectrum of complex 1.



Fig

. S7. ESI-MS spectrum of complex **1** in methanol, showing relevant peaks.

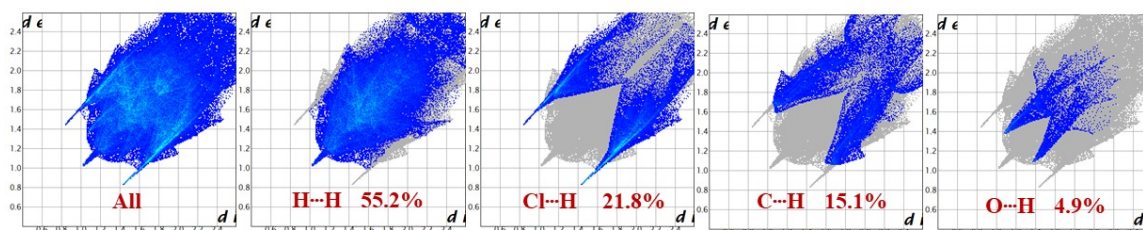


Fig. S8. 2D fingerprint plots of complex **1**.

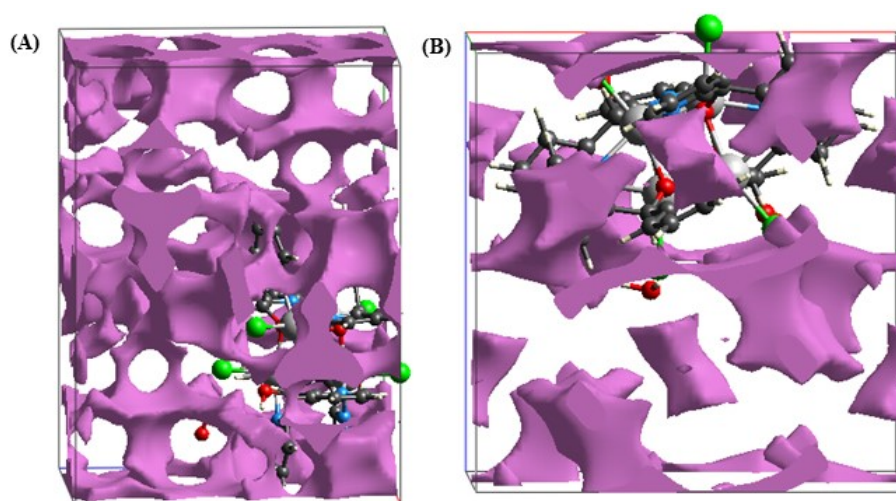


Fig. S9. Void surfaces of complex **1** arising from different isovalues (0.002 au (a) and 0.0008 au (b)) for a unit cell.

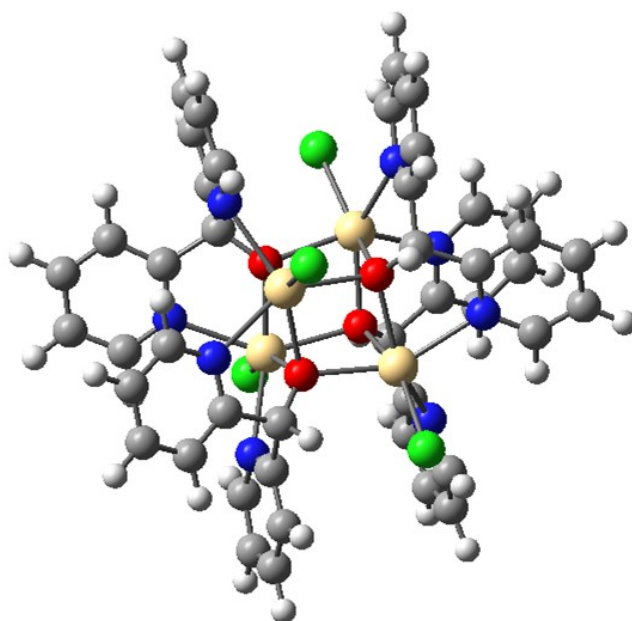


Fig. S10. DFT optimized structure of complex **1**.

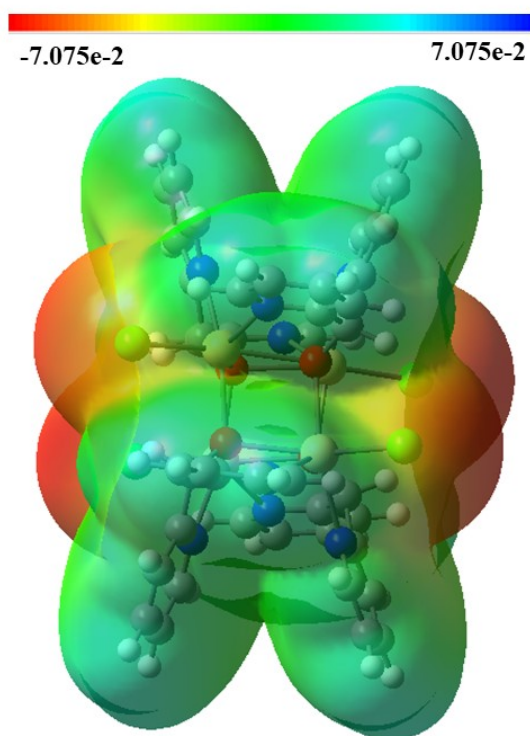


Fig. S11. Molecular electrostatic potential surface of complex **1**.

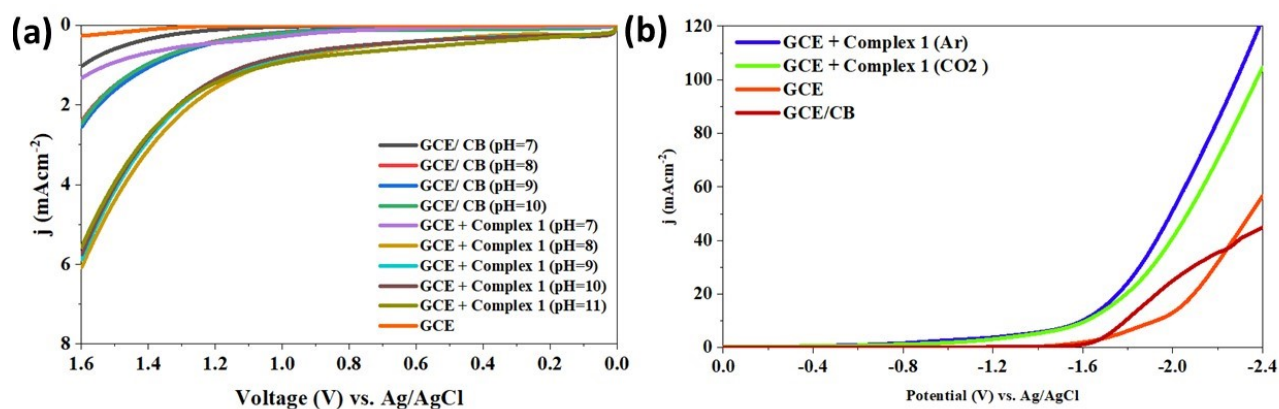


Fig. S12. LSV control experiment for (a) water oxidation and (b) CO₂ reduction activity of complex **1**.

Table S1. Interaction parameters of complex **1**.

C–H⋯π interactions				
C–H⋯Cg	H⋯Cg(Å)	C⋯Cg(Å)	C–H⋯Cg(°)	
C(6')–H(6')⋯Cg(3) ^a	2.97	3.934(17)	162	
C(6')–H(6')⋯Cg(4) ^b	2.97	3.934(17)	162	
Equivalent position codes: (a) = x, y, z, (b) = 1-x, y, 1/2-z.				
Hydrogen bonding interactions				
D–H⋯A	D–H (Å)	H⋯A (Å)	D⋯A (Å)	D–H⋯A (°)
O(3)–H(3A)⋯Cl(2) ^a	0.73(3)	2.54(3)	3.2598(17)	166(3)
O(3)–H(3B)⋯Cl(1) ^b	0.83(4)	2.45(4)	3.2540(17)	166(3)
C(2)–H(2)⋯O(3) ^c	0.95	2.58	3.333(3)	136
C(10)–H(10)⋯Cl(1) ^a	0.95	2.73	3.5357(19)	143
C(11)–H(11)⋯O(1) ^a	0.95	2.60	3.264(14)	127
C(13)–H(13)⋯O(3) ^d	0.95	2.59	3.348(2)	137
A = acceptor, D = donor; Equivalent position codes: (a) = 1/2-x, 1/2-y, 1/2+z, (b) = 1-x, y, 1/2-z, (c) = x, -y, -1/2+z, (d) = -1/2+x, 1/2-y, 1-z.				

Table S2. Hirshfeld surface properties of cadmium cubane cluster.

Compound	Volume (Å ³)	Area (Å ²)	Globularity (G)	Asphericity (Ω)
Complex 1	1174.60	687.03	0.784	0.030